AD_____

Award Number: DAMD17-01-1-0423

TITLE: Assessing Vascular Oxygen Dynamics for Breast Tumor Prognosis: Comparison Between MR BOLD and Near Infrared Method

PRINCIPAL INVESTIGATOR: Yueqing Gu, Ph.D.

CONTRACTING ORGANIZATION: The University of Texas at Arlington
Arlington, Texas 76019

REPORT DATE: September 2002

TYPE OF REPORT: Annual Summary

PREPARED FOR: U.S. Army Medical Research and Materiel Command
Fort Detrick, Maryland 21702-5012

REPORT DOCUMENTATION PAGE

Form Approved
OMB No. 074-0188

1. AGENCY USE ONLY (Leave blank)	2. REPORT DATE	3. REPORT TYPE AND DATES COVERED
	September 2002	Annual Summary (1 Sep 01 - 31 Aug 02)

4. TITLE AND SUBTITLE
Assessing Vascular Oxygen Dynamics for Breast Tumor Prognosis: Comparison Between MR BOLD and Near Infrared Method

5. FUNDING NUMBERS
DAMD17-01-1-0423

6. AUTHOR(S) :
Yueqing Gu, Ph.D.

7. PERFORMING ORGANIZATION NAME(S) AND ADDRESS(ES)
The University of Texas at Arlington
Arlington, Texas 76019

E-Mail: yueqing@uta.edu

8. PERFORMING ORGANIZATION REPORT NUMBER

9. SPONSORING / MONITORING AGENCY NAME(S) AND ADDRESS(ES)
U.S. Army Medical Research and Materiel Command
Fort Detrick, Maryland 21702-5012

10. SPONSORING / MONITORING AGENCY REPORT NUMBER

11. SUPPLEMENTARY NOTES
report contains color

12a. DISTRIBUTION / AVAILABILITY STATEMENT
Approved for Public Release; Distribution Unlimited

12b. DISTRIBUTION CODE

13. ABSTRACT ***(Maximum 200 Words)***

The goal of this research project is to investigate vascular oxygen dynamics in breast tumors by correlating the results of NIRS and BOLD in MRI. I have compared simultaneous measurements of three oxygen-related indicators (arterial hemoglobin oxygen saturation SaO_2, tumor vascular oxygenated hemoglobin concentration $[HbO_2]$, and tumor oxygen tension pO_2) by a pulse oximeter, NIRS and optic fiber needle system FOXY™, respectively. The consistence of the three oxygen-related parameters in evaluating the dynamic response of oxygen level in breast tumors to hyperoxic inspiratory treatment demonstrated the capability of NIRS as a noninvasive, real time monitoring tool for tumor vascular oxygenation. With this convinced NIRS, I monitored the dynamic responses of $[HbO_2]$ to different interventions for optimizing modalities in breast tumor treatment. Results showed that hyperoxic gases, carbogen and oxygen, can repeatedly and effectively elevate the oxygen level in breast tumors, without significant difference in magnitude of $\Delta[HbO_2]$. And hydralazine can significant reduce breast tumor vascular $\Delta[HbO_2]$, independent of gas breathing. The heterogeneity of oxygenation in breast tumors was also investigated by the multi-channel optic fiber needle system FOXY™.

14. SUBJECT TERMS
technology development, radiologic sciences, tumor therapy planning and prognosis, tumor physiology monitoring

15. NUMBER OF PAGES
48

16. PRICE CODE

17. SECURITY CLASSIFICATION OF REPORT	18. SECURITY CLASSIFICATION OF THIS PAGE	19. SECURITY CLASSIFICATION OF ABSTRACT	20. LIMITATION OF ABSTRACT
Unclassified	Unclassified	Unclassified	Unlimited

Table of Contents

2001-2002 ANNUAL PROGRESS REPORT (YEAR 1)

This report presents the specific aims and accomplishments of our breast cancer research project during the first year of funding sponsored by the U.S. Department of the Army. It covers our activities from September 1, 2001 to October 31, 2002.

Introduction

The oxygen status in breast tumor has been shown to be a pivotal factor in many aspects. Particularity, it greatly affects the efficacy of non-surgical tumor therapeutic outcomes. Selective manipulation of tumor oxygenation by a range of modifiers has been shown to be able to enhance various forms of therapy. Accordingly, accurate assessment of tumor oxygenation at various stages of tumor growth and in response to interventions may provide a better understanding of tumor development and may serve as a prognostic indicator for treatment outcome. The Blood Oxygenation Level Dependent (BOLD) signal in MRI can provide a noninvasive method for tumor oxygenation monitoring. However, interpretation of the BOLD signal is confounded by variation in hemoglobin concentration, saturation and blood flow. Near Infrared Spectroscopy (NIRS) offers a noninvasive real time monitoring way to differentiate the changes in hemoglobin saturation and concentration in breast tumors caused by respiratory intervention [1,2].

Objectives

The goal of this project is to investigate vascular oxygen dynamics in breast tumors by correlating the results of NIRS and BOLD in MRI. We wish to utilize the NIR technique for better understanding of the BOLD signal in order to improve its clinical use as a diagnostic/prognostic tool for breast cancer research and clinical practice.

The project has three specific aims:

Aim 1: To investigate heterogeneity of SO_2 in the tumor vascular bed of breast tumors, using a NIRS system against the fiber optic needle measurements.

Aim 2: To compare and correlate the measurement results of the breast tumors under 100% O_2 intervention taken simultaneously from the NIR oximeter and from the BOLD method.

Aim 3: To study the influence of five interventions on SO_2 and BOLD on breast tumors with various sizes using both the NIR oximeter and the MRI BOLD method.

Body of the Report

As mentioned above, the purpose of this project is to investigate vascular oxygen dynamics in breast tumors by correlating two methods: NIRS and BLOD in MRI. In the first year, my focus is to obtain the appropriate knowledge and skills for conducting the project (months 1-6), and to perform the measurements of vascular oxygen dynamics in breast tumors by using NIRS system combined with fiber optic needle system (FOXY)™(months 6-12). I have mainly accomplished this task, as reported below:

Accomplishments during the first period (months 1-6):

a. Obtained the skills for handing laboratory animals. Taking the animal handing class provided by the University of Texas Southwestern Medical Center at Dallas; Practicing saline injection through i.p. and i.v.

b. Gained basic understanding of tumor physiology, oxygenation and dynamic processes. Taking the

course of *Human Physiology* provided by University of Texas Southwestern Medical Center at Dallas;

c. Studied the fundamentals of MRS and MRI and performed ^{19}F MRS of PFOB measurement for blood volume (see the reportable outcomes).

d. Studied the fundamentals of NIRS and performed blood phantom experiments for evaluating the NIRS system.

NIR light (700 to 900nm), where photon transport in tissue is dominated by scattering rather than absorption, has the maximal penetration depth (several centimeters), therefore enabling *in vivo* sampling of large tissue volumes, such organs as the breast, the brain, and skeletal muscles, or deep tumors. The absorptions of NIR light by two major endogenous chromospheres, i.e., oxygenated and deoxygenated hemoglobin, HbO_2 and Hb, have been used to determine important physiological indicators: hemoglobin oxygenation and blood concentration changes[1,2]. Modified Beer-Lambert's Law is given as the following equations:

$$ln(I_o/I) = = \mu_a L \tag{1}$$

$$\begin{aligned} \mu_a^{\lambda 1} &= \varepsilon_{Hb}^{\lambda 1}[Hb] + \varepsilon_{HbO2}^{\lambda 1}[HbO_2] + \alpha^{\lambda 1} \\ \mu_a^{\lambda 2} &= \varepsilon_{Hb}^{\lambda 2}[Hb] + \varepsilon_{HbO2}^{\lambda 2}[HbO_2] + \alpha^{\lambda 2} \end{aligned} \tag{2}$$

where I_o and I are the incident and the detected optical intensities, respectively, and L is the optical path length traveled by light inside the medium, μ_a is the absorption coefficient, depending on the wavelengths, $\lambda 1, \lambda 2$ are the wavelengths of near infrared light, ε is the extinction coefficient, *[HbO_2]* and *[Hb]* are concentrations of oxygenated and deoxygenated form of hemoglobin, α is the background absorption of tissue which can be ignored.

In this project, a homodyne frequency-domain NIRS system was used to monitor the global changes of *[HbO_2]* and *[Hb]* in breast tumors during the respiratory intervention. The wavelengths of NIR light in this system are at 758nm and 785nm. Thus, the changes in oxygenated, deoxygenated hemoglobin and total hemoglobin concentrations, $\Delta[HbO_2]$ and $\Delta[Hb]$, $\Delta[Hb]_{total}$ due to respiratory intervention were derived from the measured amplitudes at the two wavelengths and calculated using the following equations:

$$\Delta[HbO_2] = \frac{-10.63 \cdot \log(\frac{A_B}{A_T})^{758} + 14.97 \cdot \log(\frac{A_B}{A_T})^{785}}{d} \tag{3}$$

$$\Delta[Hb] = \frac{8.95 \cdot \log(\frac{A_B}{A_T})^{758} - 6.73 \cdot \log(\frac{A_B}{A_T})^{785}}{d} \tag{4}$$

$$\Delta[Hb]_{total} = \Delta[HbO_2] + \Delta[Hb] \tag{5}$$

where A_B and A_T are the baseline and transient amplitudes measured from the NIR system, respectively, d is the source-detector separation.

Based on equation (3), (4) and (5), blood phantom study was conducted to evaluate the accuracy of NIRS for real time measurement of oxy- and deoxygenated hemoglobin concentrations. 100 ml of 20% intralipid (Fresenius Kabi Clayton, L.P., NC) was mixed into 1900 ml of saline to get a 2 L 1 % intralipid solution with a reduced scattering coefficient of $\mu_s' = 10\ cm^{-1}$. 2 packets of phosphate buffered saline (Sigma, St.Louis, MO) were added to adjust pH = 7.4. 14 g yeast was dissolved in the phantom solution to consume the oxygen. After the baseline measurement, 6 ml of rat blood was added into the solution twice to change the hemoglobin concentration. Oxygen was delivered into the phantom solution to

oxygenate the hemoglobin. The source and detector of the NIRS were put in a reflecting geometry (d=4 cm) for the phantom measurement. Fig.1 is the time profile of $\Delta[HbO_2]$, $\Delta[Hb]$ and $\Delta[Hb]_{total}$ during the phantom experiment. 6 ml of rat blood, added twice to the phantom solution (pH=7.4, μ_s'=10 cm^{-1}), produced the same amount of elevation in $\Delta[Hb]_{total}$. Pumping O_2 leads the deoxygenated hemoglobin to be converted into oxygenated hemoglobin, with $\Delta[HbO_2]$ reaching the maximal, and $\Delta[Hb]$ back to the baseline. After stopping O_2 pumping, yeast became the dominant to consume oxygen, letting $\Delta[HbO_2]$ go back to baseline and $\Delta[Hb]$ rise up to maximal. $\Delta[Hb]_{total}$ remained the same during the oxygen regulation. The measured $\Delta[HbO_2]$,$\Delta[Hb]$, $\Delta[Hb]_{total}$ are consistent with the expected values, validating the accuracy of NIRS for the real time measurement of $\Delta[HbO_2]$, $\Delta[Hb]$, and $\Delta[Hb]_{total}$. Using the convinced system, I performed a series of experiments on animals to investigate the dynamic response of tumor vascular oxygenation to different interventions in the second period(months 6-12).

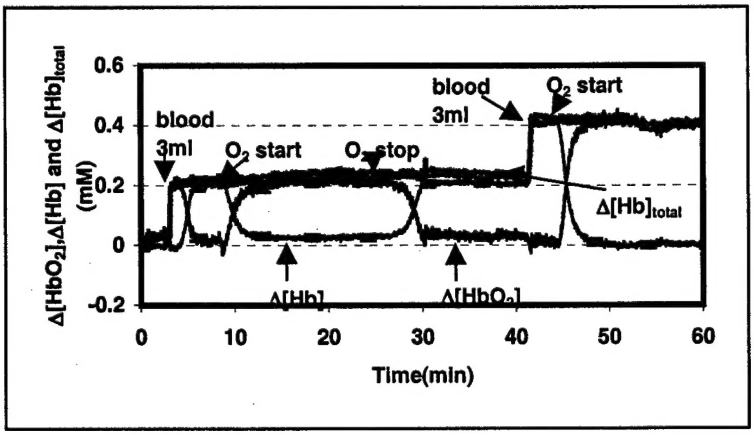

Figure 1 The profile of $\Delta[HbO_2]$, $\Delta[Hb]$, $\Delta[Hb]_{total}$ during oxygenation and deoxygenation regulation in blood phantom experiment. 6 ml of rat blood was added into 2 L of 1% intralipid solution (pH=7.4). O_2 and yeast were used to oxygenate and deoxygenate hemoglobin,respectively.

Accomplishments during the second period (months 6-12):

a. Dynamic responses of three oxygen-sensitive parameters to carbogen intervention on breast tumors

The dynamic response of tumor oxygenation to hyperoxic gas intervention may serve as a prognostic indicator for the treatment outcome. Several parameters can be used to evaluate the oxygen status. In this project,three oxygen-related parameters, i.e., arterial hemoglobin oxygen saturation, SaO_2, tumor vascular oxygenated hemoglobin concentration, $[HbO_2]$, and tumor oxygen tension, pO_2, were simultaneously measured on a group of 5 rats by a pulse Oximeter, NIRS and multi-channel optic fiber needle system $(FOXY)^{TM}$, respectively, for studying the dynamic response of tumor oxygen status to carbogen intervention (Figure 2).

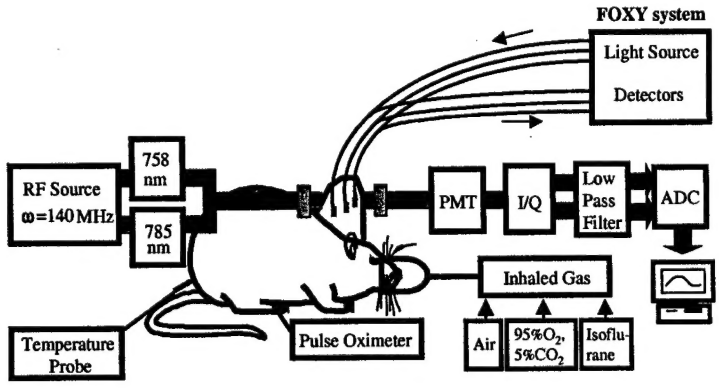

Figure 2. Schematic diagram of experimental setup for the NIR spectroscopy system, $FOXY^{TM}$ fiber optic oxygen sensor needle system and pulse oximeter.

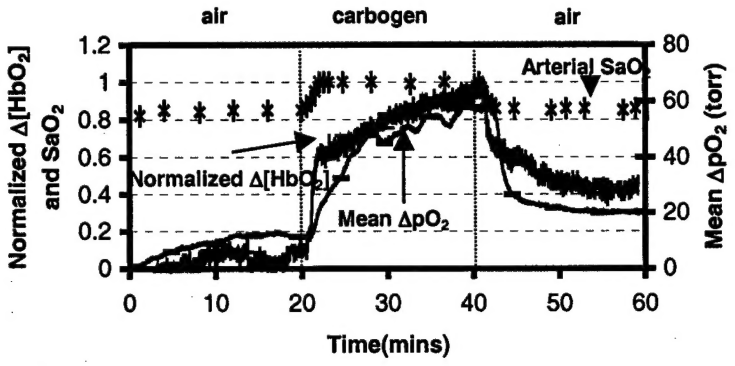

Figure 3 Time course of normalized $\Delta[HbO_2]$, mean ΔpO_2, and SaO_2 in response to carbogen intervention for a representative 13762NF breast tumor

Figure 3 shows the time profiles of the normalized $\Delta[HbO_2]$, mean ΔpO_2, and SaO_2 in response to carbogen intervention for a representative 13762NF breast tumor. All three oxygen-sensitive indicators displayed similar dynamic tendency, but different response behavior with respect to carbogen intervention. As shown in Figure 3, when the inspired gas was switched from air to carbogen, the SaO_2 readings increased rapidly from the baseline to the maximum within 2.5 minutes ($p<0.0001$), displaying a single-phase dynamic behavior. The normalized $\Delta[HbO_2]$ showed a sharp rise in the first minute ($p<0.0001$) followed by a slow, gradual, but significant increase over the next 19 minutes ($p<0.001$),

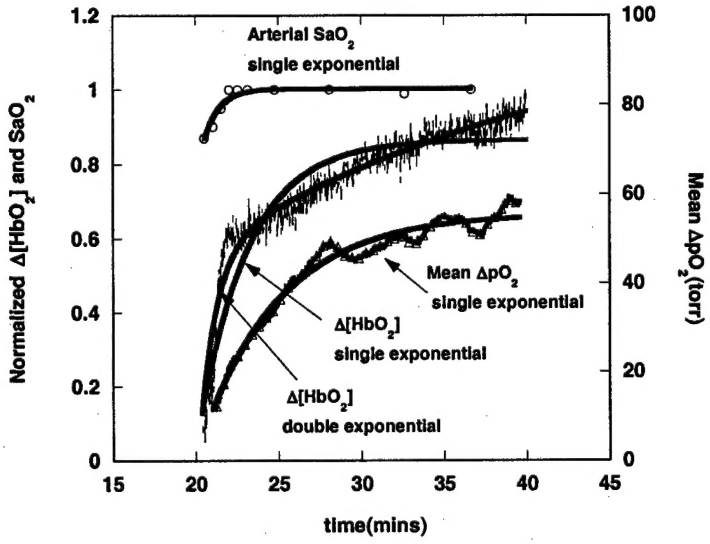

Figure 4. Response behavior of the three oxygen-sensitive parameters to carbogen intervention in the rising part. Single-exponential fittings all of the three signals, Two-exponential fitting for $\Delta[HbO_2]$.

apparent bi-phase response behavior occured. Mean ΔpO_2 displayed a quick increase within 8 minutes ($p<0.0005$) and then continued a slower and gradual increase over the next 12 minutes ($p<0.005$). Return to breathing air produced a significant decline for all three signals ($p<0.0001$). The response behaviors of the three parameters to carbogen intervention can be quantified by the time constants of exponential fitting (Figure 4). Single-exponential formula can fit SaO_2 and ΔpO_2 well, while double exponential can fit the $\Delta[HbO_2]$ better. For the fitting results, SaO_2 demonstrated a fast response, with a time constant of $\tau(SaO_2) = 1.1 \pm 0.2$ min ($R=0.93$). ΔpO_2 yielded a slower response to carbogen intervention, with a time constant of $\tau(\Delta pO_2) = 4.56 \pm 0.06$ min ($R=0.98$). The time constant in the first phase of $\Delta[HbO_2]$, $\tau_1=0.5\pm0.2$ min, has magnitudes similar to $\tau(SaO_2)$, whereas the time constant in second phase, $\tau_2= 14\pm11$ min, exhibits a large variation with respect to ΔpO_2. Data for the group of 5 rats are similar, details are

described in the attached manuscript. Results are consistent with a tumor model described by Liu et al [2], demonstrating that NIR samples the signals from small vessels within the optical field of the NIR probe. Our observation, i.e., time constants of SaO_2 are in the same order of magnitude as those of the first phase of the biphasic $\Delta[HbO_2]$, may indicate that the fast response in $\Delta[HbO_2]$, after the carbogen breathing onset, results from arterioles and capillaries in well perfused regions. Conversely, $\tau_2(\Delta HbO_2)$ has a relatively large value with a large deviation (~14±11 minutes). We may speculate that this slow, gradual elevation results from the venous or poorly perfused regions, where the vessels are much less sensitive to the intervention. The difference in time constant gave us insight into understanding of the signal acquired by NIRS and tumor physiology.

b. Heterogeneity of vascular oxygenation on breast tumors displayed by fiber optic needle system

The heterogeneity of hypoxia was pronounced in most of the solid tumors. Multi-channel fiber optic oxygen sensor needles (FOXY™) provide an alternative way to monitor tumor oxygen tension. It generally indicated distinct heterogeneity in pO_2. Moreover, responses of these pO_2 needles to hyperoxic gas were diverse: those probes integrated apparently well oxygenated regions usually showed a large response, while those with lower baseline pO_2 showed little change. Figure 5 displayed the pO_2 signals of the three channels on a representative breast tumor. For comparison with the global NIR measurements, the mean ΔpO_2 was also presented. Obviously, FOXY™ fiber optic oxygen sensing system offers an alternative means for real-time monitoring of pO_2 in tumors. Compared with the pO_2 electrode, FOXY™ system verifies the heterogeneity of tumors, with multi-probes designated in multiple regions in tumors. Furthermore, it can search for a representative high and low pO_2 baseline. But it provides very few data points compared with MRI, which can image a spatially resolved pO_2 map[3,4].

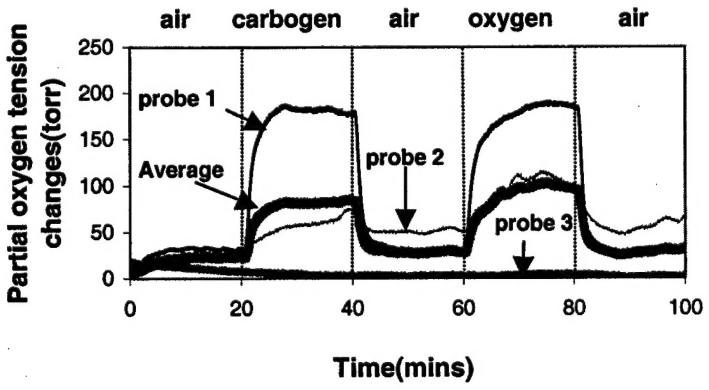

Figure 5 Time profiles of tumor oxygen tension changes, ΔpO_2, measured with the three channels of the FOXY™ fiber optic, oxygen-sensing system with respect to different gas inhalations on a breast tumor

c. Repeatability of dynamic response of breast tumors to carbogen

Inhalation of hyperoxic gases was considered to be one of the most effective methods to increase tumor oxygen status, and thus, to enhance the efficiency of standard radiotherapies in experimental malignancies as well as in human tumors[5,6]. Whether or not the vascular oxygenation can be regulated repeatedly by hyperoxic gases was demonstrated here. 8 breast tumor bearing rat models experienced repeatedly carbogen interventions with 20 minutes of air breathing as recovery, i.e., air-carbogen-air-carbogen-air. The changes of tumor vascular oxygenated hemoglobin concentrations, $\Delta[HbO_2]$, were monitored by NIR spectroscopy. Figure 6 shows the time course of $\Delta[HbO_2]$ with two intervention cycles for a representative 13762NF breast tumor. Bio-phasic response behavior, i.e.,a sharp rise in first minutes followed by a slow, gradual, but significant increase over the next period, was displayed in the group of 8 rats. Very similar response behaviors, including the magnitude of $\Delta[HbO_2]$ and dynamic response speed,

were observed in the second intervention cycle. The response behaviors, quantified by a time constant ratio (τ_2/τ_1) obtained from a double-exponential fitting, was plotted in Figure 7 for the same group of 8 rats. The variation among each pair of τ_2, τ_1 was plotted in the form of error bars. The strong linear relationship between the two intervention cycles indicated the repeatability of response behavior to carbogen intervention in all the tumors. The similarity in both magnitude of $\Delta[HbO_2]$ and dynamic response behaviors demonstrated the repeatable oxygenation of the breast tumors regulated by carbogen, and 20 minute air breathing is suitable for re-equilibration in each inhalation period.

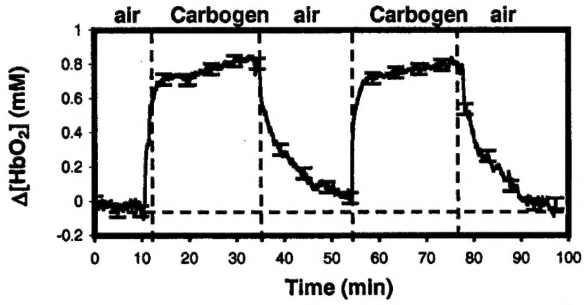

Figure 6 Time course of tumor vascular $\Delta[HbO_2]$ for a representative 13762NF breast tumor , with the inhaled gas under the sequence of air-carbogen-air-carbogen-air.

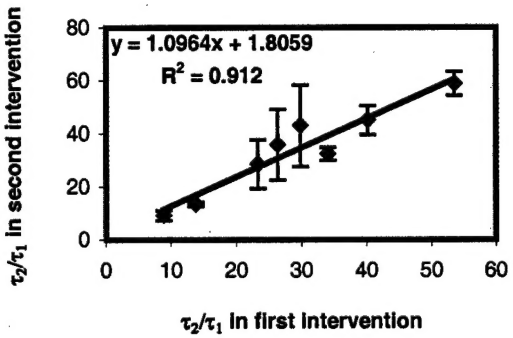

Figure 7 Relationship of the time constant ratios, τ_2/τ_1, between the two intervention cycles among the 8 rat tumors. τ_1 and τ_2 are the time constants in the first and second phase of $\Delta[HbO_2]$, respectively.

d. Comparison of oxygen and carbogen on breast tumor vascular oxygenation

Carbogen has been favored over oxygen as an adjuvant intervention to enhance non-surgical therapy, and it has been suggested that oxygen breathing is less effective due to hypotension. However, studies on experimental tumors in animals as well as on clinical trials in patients have shown non-uniform results, concerning the therapeutic benefit of the two kinds of respiratory hyperoxic gases[7,8]. In this project, two groups of rats (seven rats in each group), were exposed to two different gas inhalation sequences, i.e., air-carbogen-air-oxygen-air and air-oxygen-air-carbogen-air, with a temporal interval of 20 minutes between gas switches, to compare the effects of carbogen and oxygen interventions on $\Delta[HbO_2]$. The results have shown that both carbogen and oxygen can significantly improve the oxygen status of the tumors without significant difference in the magnitude of $\Delta[HbO_2]$. However, the dynamic responses are different and depend on the gas inhalation sequence. In the sequence of air-carbogen-air-oxygen-air, with carbogen prior to oxygen, strong bi-phasic responses of $\Delta[HbO_2]$ to carbogen intervention were displayed in all the tumors, but disappeared in most of the cases with the 'reversed' breathing sequence. Oxygen produced mono-phasic response behavior in most of the cases.(see attached manuscript in detail).

e. Study the effect of hydralazine on oxygenation and total hemoglobin concentration

In contrast to hyperoxic gas inhalation, hydralinze administration may increase tumor hypoxia, and thus, enhance the efficacy of oxygen-dependent chemotherapy[9,10]. In this project, hydralinze was intravenously administrated into the blood stream of 8 breast tumor bearing rats to study the effect of hyrdalazine on tumor vascular $\Delta[HbO_2]$ and $\Delta[Hb]_{total}$. Figure 8 is the time profile of $\Delta[HbO_2]$ and $\Delta[Hb]_{total}$ in response to different gas inhalations and hydralazine administration on a representative breast

tumor. Carbogen and oxygen can significantly elevate tumor vascular oxygenation, while hydralazine significantly reduce the tumor oxygenation and total hemoglobin concentration. The results for all of the 8 rat tumors demonstrated that hydralinze has the ability to decrease the tumor oxygen level and total hemoglobin concentration significantly, and thus enhance the efficacy of some chemotherapy. To study the possible effect of breathing gas, hydralinze was administrated under air breathing for another group of 8 rats. Fig. 9 is the time course of $\Delta[HbO_2]$ and $\Delta[Hb]_{total}$ under different gas inhalations and hydralinze administration for representative breast tumor. Results demonstrated that hydralazine can significantly reduced the tumor oxygenation and total hemoglobin, independent of breathing gases.

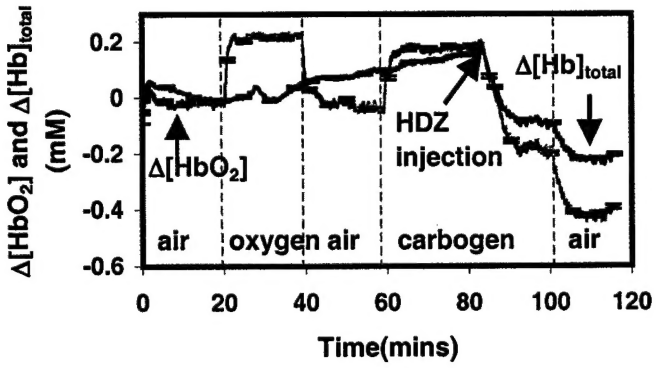

Figure 8 Time course of tumor vascular $\Delta[HbO_2]$ and $\Delta[Hb]_{total}$ for a representative 13762NF breast tumor with the inhaled gas under the sequence of air-oxygen-air-carbogen-air. Hydralazine was administrated under carbogen breathing.

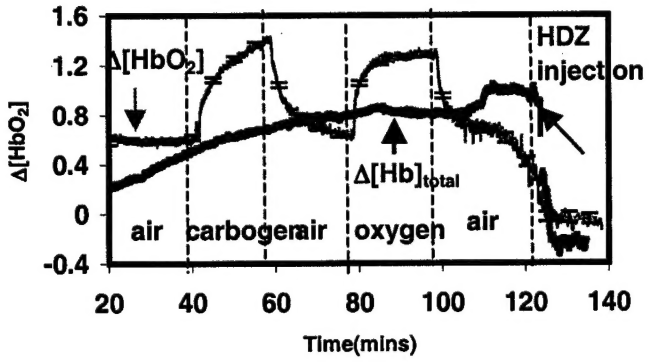

Figure 9 Time course of tumor vascular $\Delta[HbO_2]$ and $\Delta[Hb]_{total}$ for a representative 13762NF breast tumor with the inhaled gas under the sequence of air-carbogen-air-oxygen--air. Hydralazine was administrated under air breathing.

Key Accomplishments:

- **a.** Obtained the mainly knowledge and skills for conducting this project. (training in handling laboratory animals, studying the fundamentals and operation in the NIR oximeter and MRS or MRI BOLD method.)
- **b.** Investigated the relationships among the three oxygen-sensitive parameters, ie, arterial oxygen saturation, tumor vascular hemoglobin concentration, and tumor oxygen tension. All the three parameters showed similar trendy with respect to carbogen intervention, but different response time constant, which provides a deep insight of NIR signal and tumor physiology.
- **c.** Studied the heterogeneity of breast tumors by multi-channel optical fiber needle system (FOXY™). This system offered an alternative way for real time monitoring the pO_2 and their responses to interventions in different regions.

d. Investigated the dynamic response of tumor vascular $\Delta[HbO_2]$ to different interventions, ie., carbogen, oxygen inhalation and hydralazine administration. Results indicated that breast tumor vascular oxygenation can be regulated repeatedly by hyperoxic gases, with 20 minutes gas breathing for re-equilibration. Both carbogen and oxygen can elevate tumor oxygenation significantly, without difference in magnitude of $\Delta[HbO_2]$; Hydralazine can significantly reduce tumor oxygenation and total hemoglobin, independent of gas breathing . These results provide important information for optimizing modalities in breast tumor treatment.

Reportable Outcomes

Manuscripts for Peer-reviewed Journals:

1. Y.Gu, V.Bourke, J.Kim, A.Constantinescu, R.P.Mason, H.Liu, "Dynamic response of breast tumor oxygenation to hyperoxic respiratory challenge monitored with three oxygen-sensitive parameters", Submitted to *Applied Optics.*
2. Y.Gu, H.Liu, A.Constantinescu, R.P.Mason, " Breast tumor vascular dynamics: non-invasive monitoring by NIRS" in preparation and will be submitted to *Cancer Research*

Presentations and Proceeding papers:

1. Y.Gu, Y.Song, A.Constantinescu, R.P.Mason, H.Liu "Correlation between tumor vascular total hemoglobin concentration and blood volume measured by NIR spectroscopy and ^{19}F MRS of PFOB" Oral presented in OSA Biomedical Topical Meetings sponsored by Optical Society of American, in Maimi, Fl, April 7~9(2002)

2. Y.Gu, V.Bourke, J.Kim, A.Constantinescu, R.P.Mason, H.Liu "Dynamic response of breast tumor oxygenation to hyperoxic respiratory challenge monitored by NIR Spectroscopy " presented in the Breast Cancer Research meeting sponsored by the U.S.Army Medical Research Material Command in Orlando, FL, Sept.26~30 (2002).

Conclusions

From the work that I have conducted up-to-data, three conclusions can be drawn as the following:

a. The dynamic responses of three oxygen-related indicators, i.e, arterial oxygen saturation, tumor vascular hemoglobin concentration, and tumor tissue oxygen tension, are consistence in evaluating the oxygen level changes in breast tumors under carbogen intervention. The results demonstrated the capability of NIR spectroscopy as a noninvasive, real time monitoring tool for tumor vascular oxygneation. The bi-phasic behavior of $\Delta[HbO_2]$ implies that the signal in the fast phase results from the arterial and well perfused regions, and the signal in the slow phase results from the venous and poor perfused regions.
b. Hyperoxic gases, carbogen and oxygen, can effectively manipulate the oxygen level in breast tumor, without significant difference in magnitude of $\Delta[HbO_2]$. 20 minutes gas breathing is suitable for re-equilibration of the rats.
c. Hydralazine can significant reduce the vascular oxygenation and total hemoglobin concentration in breast tumors, independent of gas breathing. These results imply that chemotherapy is an alternative way for the treatment of breast tumors.

Reference

[1] E.L.Hull, D.L. Conover, and T.H. Foster, "Carbogen induced changes in rat mammary tumor oxygenation reported by near infrared spectroscopy," Br.J.Cancer. 79,1709-1716 (1999).

[2] H.Liu, Y.Song, K. L.Worden, X.Jiang, A.Constantinescu, and R.P.Mason, " Noninvasive investigation of blood oxygenation dynamics of tumors by near-infrared spectroscopy," Appl. Opt. 39,5231-5243 (2000).

[3] R.P.Mason, P.P.Antich, E.E.Babcock, A.Constantinescu, P.Peschke, E.W.Hahn, "Noninvasive determination of tumor oxygen tension and local variation with growth," Int.J.Radiat. Oncol. Biol.Phys. 29,95-103 (1994).

[4] D.Zhao, A.Constantinescu, L.Jiang, E.W.Hahn, R.P.Mason, "Prognostic radiology:quantitative assessment of tumor oxygen dynamics by MRI," Am. J. Clin Oncol. 24(5),462-466 (2001).

[5] S. Dische, "What we learnt from hyperbaric oxygen?" Radiother oncol.20(suppl),71-74(1991)

[6] V.M.Laurence, R.Ward, I.F.Dennis, N.M.Bleehen, "Carbogen breathing with nicotinamide improves the oxygen status of tumors in patients," Br. J Cancer,72,198-205 (1995).

[7] S.Dische, M.I.Saunders, R.Sealy, "Carcinoma of the cervix and the use of hyperbaric oxygen with radiotherapy:a report of a randomized controlled trial," Radiother Oncol.53,93-98 (1999).

[8] L.Martin, E.Lartigau, P.Weeger, "Changes in the oxygenation of head and neck tumors during carbogen breathing," Radiother Oncol,27,123-130 (1993).

[9] B. M.Fenton, " Influence of hydralazine administration on oxygenation in spontaneous and transplanted tumor models", Int.J.Radiation Oncology Biol.Phys., vol 49, No.3, 799-808 (2001).

[10] D.G.Hirst, V.K. Hirst, K.M.Shaffi. V.E.Prise and B. Joiner. "The influence of vasoactive agents on the perfusion of tumours growing in three sites in the mouse?" Int.J. Radiat. Biol. 60 ,211-218 (1991).

Appendix

Manuscript submitted to *Applied Optics*

Dynamic Response of Breast Tumor Oxygenation to Hyperoxic Respiratory Challenge Monitored with Three Oxygen-Sensitive Parameters

Yueqing Gu, Vincent Bourke*, Jae Kim,

Anca Constantinescu*, Ralph P. Mason*, Hanli Liu

Biomedical Engineering graduate program, University of Texas at Arlington, TX76019

*Dept. of Radiology, University of Texas Southwestern Medical Center, Dallas, TX75390

Corresponding author: Hanli Liu

Biomedical Engineering graduate program,

The University of Texas at Arlington, TX76019

501 west first, ELB-220, P.O.Box 19138

email: Hanli@uta.edu

Tel: 817-272-2054

Fax: 817-272-2251

Abstract

The ability of Near Infrared Spectroscopy (NIRS) to monitor therapeutic interventions for rat breast tumors *in-vivo* in real time is demonstrated. We compared simultaneous measurements of three oxygen-sensitive parameters (arterial hemoglobin oxygen saturation (SaO_2), tumor vascular oxygenated hemoglobin concentration ($[HbO_2]$), and tumor oxygen tension (pO_2)) to evaluate dynamic responses of breast tumors to hyperoxic respiratory challenges. All three parameters displayed similar trends in dynamic response to carbogen (5% CO_2 and 95% O_2) intervention, but with different response times. These response times were quantified by the time constants of the exponential fitting curves, revealing the immediate and the fastest response from the arterial SaO_2, followed by biphasic changes in tumor vascular $[HbO_2]$, and delayed responses for pO_2. The biphasic dynamic characteristic for changes of $[HbO_2]$ implies two different perfusion rates/mechanisms in the tumor vasculature. The effects of two hyperoxic gases (carbogen and oxygen) were compared, using two groups of Fisher rats and two different gas inhalation sequences, i.e., air-carbogen-air-oxygen-air and air-oxygen-air-carbogen-air. The results demonstrate that both of the inhaled, hyperoxic gases can significantly improve the tumor oxygen status. However, the biphasic response of $\Delta[HbO_2]$ with carbogen intervention was not seen in the "reverse" inhalation sequence. Heterogeneous responses to hyperoxic interventions in the tumor were displayed by the pO_2 signals measured in different regions of the tumor.

OCIS codes: 170.1470, 170.3660, 170.4580, 120.3890, 120.1880, 230.2090.

1.Introduction

It is generally recognized that hypoxic or even anoxic regions in solid- growing tumors may limit the efficacy of non-surgical therapy, including radiotherapy, photodynamic therapy, chemotherapy[1,2,3,4]. Tumor hypoxia is thought to be diffusion-limited (chronic hypoxia) or perfusion-limited (acute hypoxia). In approximately 30-60% of human tumors, oxygen deficiencies can be found, which presumably result from an insufficient O_2 supply to the tissue, and are mainly influenced by the arterial oxygen content and efficacy of perfusion in tumor tissue. In order to improve the efficacy of oxygen-dependent treatment modalities, tumor hypoxia may be reduced either by increasing the O_2 supply or by reducing the O_2 demand in the tumor cells. Inhalation of hyperoxic gas mixtures has been shown to be an effective method in achieving this goal, and thus may enhance the efficiency of the non-surgical treatment[5,6,7]. Accordingly, accurate assessment of tumor oxygenation at various stages of tumor growth and in response to interventions may provide a better understanding of tumor development and may serve as a prognostic indicator for treatment outcome, potentially allowing therapy to be tailored to individual characteristics.

In this context, many techniques have been developed to measure oxygen tension (pO_2) or vascular oxygenation of tumors[8]. Microelectrodes or mass spectrometry probes measure pO_2 directly, but they are highly invasive and often fragile[9,10]. Various other techniques of detecting tumor hypoxia require biopsy, such as cryospectrophotometry to asses hemoglobin saturation, or histology following the infusion of hypoxia labels such as pimonidazole or EF5[11,12,13]. Non-invasive variations of these approaches are under development using PET or NMR sensitive derivatives. Nuclear magnetic resonance provides an alternative noninvasive technology to estimate pO_2 directly based on the ^{19}F NMR spin lattice relaxation rates of perfluorocarbons such

as hexafluorobenzene [14,15]. Near infrared (NIR) spectroscopy offers a *non-invasive*, real-time monitoring means for tumor hemoglobin oxygenation, based on the absorption of the endogenous chromophores, i.e., oxygenated and deoxygenated hemoglobin[16,17]. Comparisons among diverse techniques to evaluate tumor oxygenation provide greater insight to optimize the therapy for human patients.

In this study, we performed simultaneous measurements of three oxygen-related parameters, i.e., arterial hemoglobin oxygen saturation, SaO_2, tumor vascular oxygenated hemoglobin concentration, $[HbO_2]$, and tumor oxygen tension, pO_2, to assess dynamic responses of rat breast tumors to hyperoxic gases. Changes in tumor vascular $[HbO_2]$ were measured by near infrared spectroscopy (NIRS) using a photon-migration, frequency-domain device, changes in regional pO_2 of the tumors were monitored by a fluorescence-quenched, oxygen-sensing, fiber optic system (FOXY)^{TM}, and the arterial SaO_2 values were recorded using a fiber-based, pulse oximeter. The responses of the three oxygen-related parameters to different gas inhalations were studied, specifically, the effects of carbogen and oxygen interventions.

2.Material and Methods

2.1 NIRS system for measurement of changes in $[HbO_2]$

NIR light (700 to 900 nm), where photon transport in tissue is dominated by scattering rather than absorption, has considerable penetration depth (several centimeters), therefore enabling *in vivo* sampling of large tissue volumes, e.g., breast, brain, skeletal muscles, or tumors. The absorptions of NIR light by oxygenated and deoxygenated hemoglobin have been used to determine important physiological indicators: hemoglobin oxygenation and blood concentration changes. In this study, a homodyne frequency-domain system (NIM, Philadelphia, PA) was used

to monitor the global changes in oxygenated and deoxygenated hemoglobin concentrations, [HbO_2] and [Hb], respectively, in rat breast tumors in response to different gas interventions. The light from two NIR laser diodes at 758 nm and 785 nm was coupled into a bifurcated fiber bundle and illuminated on the tumor. After being absorbed and scattered through the tumor tissue, the transmitted light was collected by another fiber bundle and propagated to a photomultiplier tube (PMT). The signal from the PMT was processed through an In-phase and Quadrature-phase circuit, and the amplitude changes caused by tumor tissue were recorded. Based on modified Beer-Lambert's law[18], changes in oxygenated and deoxygenated hemoglobin concentrations, $\Delta[HbO_2]$ and $\Delta[Hb]$, due to respiratory intervention were derived from the measured amplitudes at the two wavelengths and calculated using the following equations[19]:

$$\Delta[HbO_2] = \frac{-10.63 \cdot \log(\frac{A_B}{A_T})^{758} + 14.97 \cdot \log(\frac{A_B}{A_T})^{785}}{d}, \quad (1)$$

$$\Delta[Hb] = \frac{8.95 \cdot \log(\frac{A_B}{A_T})^{758} - 6.73 \cdot \log(\frac{A_B}{A_T})^{785}}{d}, \quad (2)$$

where A_B and A_T are the baseline and transient amplitudes measured from the NIR system, respectively, "d" is the source-detector separation, the unit for both $\Delta[HbO_2]$ and $\Delta[Hb]$ is mM/DPF, and DPF is the differential path-length factor for tumor tissues. The four coefficients in the equations were derived using the extinction coefficients of Hb and HbO_2 at corresponding wavelengths and corrected for the pathlength differences at the two wavelengths[19]. These two equations associate the amplitudes measured from the NIR system to the oxygen status indicators, $\Delta[HbO_2]$ and $\Delta[Hb]$, in tumors during the respiratory challenge. As demonstrated in our previous study, normalization of $\Delta[HbO_2]$ and $\Delta[Hb]$ to their maximal values can eliminate the effects of "d" and DPF on the results. [19]

Figure 1 shows the diagram of the NIR system. The delivering and detecting fiber bundles of the NIRS were placed horizontally on the surface of the tumors in a transmittance mode. The two bundle tips were placed around the middle of the tumors vertically. Thus, the current setup of the probes provides an optimal geometry for the NIR light to interrogate deep tumor tissue, and thus, to obtain a global signal from the tumor. The details of the system were previously described [18,19].

2.2 FOXY™ fiber optic oxygen sensing system for measurement of changes in pO_2

Regional pO_2 in tumors was monitored using a multi-channel, fiber optic, oxygen-sensing system (FOXY™, Ocean Optics Inc.). Three fluorescence-quenched, optical fiber probes were inserted into different regions of the tumors to monitor the changes of oxygen tension (ΔpO_2) in response to the respiratory challenges, as shown in Fig.1. Probes were positioned so that at least one was in a relatively poorly oxygenated region and at least one in a relatively well oxygenated region. An average value of the three signals was taken as a mean ΔpO_2 of the tumor. For a typical FOXY™ channel, the light emitted from a pulsed blue LED at ~475 nm was coupled into one branch of a bifurcated optical fiber bundle and propagated to the FOXY™ probe tip. Each probe is aluminum-jacketed, containing two optical fibers with 300 μm core diameter, and designed to couple to the bifurcated fiber bundle. The distal end of the probes is coated with a thin layer of a hydrophobic sol-gel material, containing an oxygen-sensing ruthenium complex trapped within the sol-gel matrix, effectively immobilized and protected from water. The ruthenium complex at the probe tips was excited by the light from the blue LED and emitted fluorescence at about 600 nm. If the excited ruthenium complex encounters an oxygen molecule, the excess energy is transferred to the oxygen molecule in a non-radiative transition, decreasing or quenching the

fluorescence signal. The degree of quenching correlates to the level of oxygen concentration or the pO_2 value in the film, which is in dynamic equilibrium with the pO_2 value in the sample. The fluorescence is collected by the probe and carried through the other branch of the bifurcated fiber to the spectrometer. Post processing of the data is accomplished by the software supplied by the vendor.

The fluorescence response of the ruthenium crystal complex is highly temperature dependent, so probe calibration was accomplished by streaming gases of known oxygen concentrations (100%, 20.9%, 10%, 2%, and 0%) through a cylindrical water jacket heated to 37 ^{0}C. Calibration curves were automatically calculated by the vendor-supplied software, using the second-order, polynomial calibration:

$$\frac{I_0}{I} = 1 + K_1 \times [O] + K_2 \times [O]^2 \qquad (3)$$

where, I_0 is the fluorescence intensity at zero concentration (nitrogen), I is the measured intensity of fluorescence at a pressure p of oxygen, [O] represents the oxygen concentration (related to pO_2), K_1 and K_2 are the first- and second- order coefficients, which are automatically supplied by the software curve fitting routine based on the calibration measurements. After the system calibration, the oxygen concentration in tumor/tissue sample measurements can be deduced using equation (3).

2.3 Pulse oximeter for measurement of arterial S_aO_2

To compare with temporal characteristics of tumor vascular oxygen dynamics in response to respiratory challenges, the systemic arterial SaO_2 of the breast tumor bearing rats was also monitored by a fiber-optic, pulse oximeter (Nonin Medical, Inc., Plymouth, MN) placed on the hind foot of the rats. The data were sampled manually.

2.4 Animal model

Mammary adenocarcinomas 13762NF (originally obtained from DCT, NIH) were implanted in skin pedicles[20] on the foreback of adult female Fisher 344 rats (~150 g). Once the tumors reached 1~2 cm diameter, rats were anesthetized with 150-μl ketamine hydrochloride (100 mg/ml,i.p.) and maintained under general gaseous anesthesia with 1.3% isoflurane in air(1 dm^3/min). Tumors were shaved to improve optical contact for NIR transmitting light, and the body temperature was maintained at 37 ^{0}C by a warm water blanket. The tumor diameters along the three major orthogonal axes (a,b,c) were measured to determine the volume of the tumor by using an ellipsoid approximation with the formula: $V=(\pi/6).a.b.c.$

In this study, two groups of rats (seven rats in each group), were exposed to two different gas inhalation sequences, i.e., air-carbogen-air-oxygen-air and air-oxygen-air-carbogen-air, with a temporal interval of 20 minutes between gas switches, to compare the effects of carbogen and oxygen on vascular oxygenation of breast tumors. For five rats in the first group, we performed the dynamic response measurements of the three oxygen-related parameters simultaneously.

3. Results

3.1 Dynamic responses of three oxygen-related parameters to carbogen intervention.

Using the setup in Fig.1, all three parameters were monitored simultaneously. Figure 2 shows the time profiles of the normalized $\Delta[HbO_2]$, mean ΔpO_2, and SaO_2 in response to carbogen intervention for a representative 13762NF breast tumor (No.1, 3.2 cm^3). When the inspired gas was switched from air to carbogen, the SaO_2 readings increased rapidly from the baseline value of 85% to the maximum of 100% within 2.5 minutes ($p<0.0001$). The normalized $\Delta[HbO_2]$ showed a sharp rise in the first minute ($p<0.0001$) followed by a slow, gradual, but significant

increase over the next 19 minutes ($p<0.001$). Mean ΔpO_2 displayed a quick increase of about 50 Torr from the baseline value within 8 minutes ($p<0.0005$) and then continued a slower and gradual increase over the next 12 minutes ($p<0.005$). Return to breathing air produced a significant decline for all three signals ($p<0.0001$).

All three oxygen-sensitive indicators displayed similar dynamic tendency in response to carbogen intervention, but notable differences among the dynamic responses of the three parameters were seen. As shown in Figure 2, SaO_2 displayed a single-phase dynamic behavior in response to carbogen intervention, while $\Delta[HbO_2]$ demonstrated an apparent bi-phasic behavior. The response differences of the three parameters to carbogen intervention can be quantified by the response time constant. For comparison among the three oxygen-related parameters, a single-exponential fitting was applied to all of them, although $\Delta[HbO_2]$ possessed a strong bi-phasic appearance (Figure 3). For the fitting results, SaO_2 demonstrated the fastest response, with a time constant of $\tau(SaO_2) = 1.1 \pm 0.2$ min ($R=0.93$). ΔpO_2 yielded the slowest response to carbogen intervention, with a time constant of $\tau(\Delta pO_2) = 4.56 \pm 0.06$ min ($R=0.98$), and $\Delta[HbO_2]$ gave an global response with $\tau(\Delta[HbO_2]) = 2.59 \pm 0.06$ min ($R=0.89$). Time constants of the three parameters for the group of five 13762NF rat breast tumors are listed in Table I. $\tau(SaO_2)$ - $\tau(\Delta[HbO_2])$ and $\tau(\Delta pO_2)$ - $\tau(\Delta[HbO_2])$ were also calculated and depicted in Figure 4. The values of $\tau(SaO_2)$ - $\tau(\Delta[HbO_2])$ were found to be negative for all five tumors, indicating that $\tau(SaO_2) < \tau(\Delta[HbO_2])$. Conversely, the ΔpO_2 response to gas intervention was slower than $\Delta[HbO_2]$, yielding positive differences in $\tau(\Delta pO_2)$ - $\tau(\Delta[HbO_2])$, as shown in Figure 4. No apparent relationship between the time constants and tumor volume was observed.

To better understand and quantify the dynamic features of $\Delta[HbO_2]$, a double-exponential expression with two time constants, τ_1 and τ_2, was also used to fit the $\Delta[HbO_2]$ data in the rising

part during carbogen intervention, yielding an improved regression fit, R. A two-exponential fitted curve is plotted in Figure 3, giving time constants of $\tau_1 = 0.61\pm0.03$ min and $\tau_2 = 21\pm3$ min for the first and second phase, respectively (R=0.97) for tumor #1. Data for other breast tumors are also provided in Table I. In comparison between the two-exponential fitting for $\Delta[HbO_2]$ and the single-exponential results for both SaO_2 and ΔpO_2 in the first five rat tumors, the time constants of SaO_2 (~1.2±0.4 min) have magnitudes similar to those of the first phase of the biphasic $\Delta[HbO_2]$ (~0.5±0.2 min), whereas the second phase of $\Delta[HbO_2]$ exhibits a large variation in time constant (~14±11 min) with respect to ΔpO_2 (~ 4±1 min), as shown in Table I.

Time delay, t_d, between the time when the gas intervention was initiated and the time when the changes in signals were detected, reviewed another difference among the three oxygen-sensitive parameters. For tumor #1 (Fig.2), when the inspired gas was switched from air to carbogen, the SaO_2 signal was the first to display the response to the intervention. Then, change in $\Delta[HbO_2]$ was observed 30 seconds later with t_d=30 sec, followed by changes in ΔpO_2 another 30 seconds later (t_d=60 sec). Similarly, when the gas was returned from carbogen to air, the SaO_2 signal decreased immediately, followed by declines in $\Delta[HbO_2]$ and in ΔpO_2 with t_d=0.5 and 2 minutes later, respectively. To clearly demonstrate the inter-relationships among these time delays, the differences in the time delays, $t_d(SaO_2)$ - $t_d(\Delta[HbO_2])$ and $t_d(\Delta pO_2)$ - $t_d(\Delta[HbO_2])$, were calculated for both rising and falling periods in the first five tumors and plotted in Figure 5. As expected, the time delays of SaO_2 to $\Delta[HbO_2]$ were negative, and the delays of ΔpO_2 to $\Delta[HbO_2]$ were positive.

3.2 Comparison of the effects of carbogen and oxygen intervention on tumor oxygenation

To compare the effects of carbogen and oxygen intervention on tumor oxygenation, two groups of rats were subjected to alternating gases with air breathing as recovery. Seven rats in the first group (including the five rats used in section 3.1) were exposed to oxygen after carbogen intervention. Figure 6 shows the time course of $\Delta[HbO_2]$ during an alternating carbogen and oxygen intervention for a representative 13762NF breast tumor (No.2, 3.0 cm^3). As described in section 3.1,the $\Delta[HbO_2]$ data showed a bi-phasic response to carbogen, i.e., a sharp increase in the first phase followed by a gradual significant elevation in the second phase. Switching back to air caused $\Delta[HbO_2]$ to decline. After 20 minutes of air breathing for re-equilibration, the rat was exposed to oxygen for another 20 minutes and then air breathing for the recovery again. Oxygen produced an abrupt increase in $\Delta[HbO_2]$ to the maximal value within 2 minutes, followed by a plateau, and then the signal decreased rapidly during the air breathing recovery. Both carbogen and oxygen inhalation significantly elevated the oxygen level in all the seven tumors.

However, while all 7 tumors showed strongly biphasic behavior with carbogen intervention, a mono-exponential gave a good fit for the data with oxygen intervention. The double-exponential fitting for the oxygen intervention produced excessive large errors for the time constant in the second phase. Fig. 7 illustrated the fitting results for both carbogen and oxygen intervention in the rising part of tumor #2 (3.0 cm^3): in the case of carbogen intervention, the time constants are τ_1 = 0.62±0.06 min and τ_2 = 11±1 min (R=0.96) for the double-exponential fitting, τ = 3.40±0.07 min (R=0.91) for the single-exponential fitting; in the case of oxygen intervention, τ = 0.51±0.01 min (R=0.91) for the single-exponential fitting. The time constants for the rest of the tumors are listed in Table I. In addition, there was no significant difference (P>0.3) in the maximal magnitude of $\Delta[HbO_2]$ between carbogen and oxygen interventions (Figure 8).

In order to examine the possible effect of preconditioning, another 7 rats experienced a "reversed" gas intervention, with exposure to oxygen prior to carbogen. Figure 9 is the time profile of normalized tumor vascular $\Delta[HbO_2]$ for a representative tumor (No.9, 2.6 cm^3). With the gas breathing sequence reversed, changes in $\Delta[HbO_2]$ with oxygen breathing (~0.8±0.1) were again not significantly different from those with carbogen (~ 0.7±0.1) for the seven rat tumors (Figure 10) ($P>0.5$). However, the time constants were now similar for both gas challenges, and carbogen no longer induced the biphasic behavior in 6 of 7 tumors.

3.3 Heterogeneity of the tumors

The FOXY™ oxygen-sensing probes generally indicated distinct heterogeneity in pO_2. Moreover, response to the hyperoxic gas was diverse: those probes that indicated apparently well-oxygenated regions usually showed a large response, while those with lower baseline pO_2 showed little change (Fig.11). For comparison with the global NIR measurements, the mean ΔpO_2 was also presented.

4. Discussion

In this study, we have simultaneously measured arterial hemoglobin oxygen saturation, SaO_2, global changes in oxygenated hemoglobin concentration of tumor vasculature, $\Delta[HbO_2]$, and regional changes in oxygen tension of tumor tissue, ΔpO_2, in response to hyperoxic gas (i.e., carbogen and oxygen) interventions using a pulse oximeter, an NIRS system and a multi-channel, fiber optic, oxygen-sensing system, respectively. All three oxygen-sensitive indicators displayed similar dynamic tendency in response to carbogen intervention (Fig.2).

The simultaneous measurements demonstrated the compatibility of the NIRS system with the FOXY™ fiber optic oxygen-sensing system, without interference from one another. The NIRS system offers a real-time measurement of $\Delta[HbO_2]$ in tumor vasculature, sampling the signals from all vessels, including arterial, capillary, and venous blood, within the optical field of the NIR probes, while the multi-channel FOXY™ fiber optic system monitors the ΔpO_2 in specific locations in tumors in real time. The compatibility of the two systems provides an opportunity to acquire HbO_2 and pO_2 signals simultaneously, leading to a valuable insight of the dynamic relationship between the blood oxygenation and tissue oxygenation of the tumors. Furthermore, the consistency of the three oxygen-related parameters in response to the hyperoxic gas interventions supports the practicability of the NIRS system as a noninvasive, real-time monitoring tool for global changes in tumor vascular oxygenation. Whether the quantity of HbO_2 determined with this methodology will be a clinically useful predictor for tumor response to oxygen-dependent interventions and therapies remains to be determined. Nevertheless, the attractive features of the NIRS system being completely non-invasive and in real time make it potentially useful in biomedical research and perhaps useful in clinical application.

The fact that dynamic response times are insensitive to geometric details and boundary conditions[21] permits the dynamic comparison of the global ΔHbO_2 and regional ΔpO_2, focusing on the time required for a given transient process to be effectively complete. The time constant analysis indicated that $\Delta[HbO_2]$ signal possessed a strong bi-phasic characteristic with carbogen intervention, while SaO_2 and ΔpO_2 can be fitted well with single-exponential expression (Fig.3 & Table I). It is known that NIRS samples the signals from very small vessels[22] within the optical field of the NIR probes. Our observation in this study that the time constants of SaO_2 are in the same order of magnitude as those of the first phase of the biphasic $\Delta[HbO_2]$ may indicate that the

fast response in $\Delta[HbO_2]$, after the carbogen breathing onset, results from arterioles and capillaries in well perfused regions. Both of the $\tau(SaO_2)$ and $\tau_1(\Delta HbO_2)$ values showed consistency among different tumors with small deviations (Table I). An ANOVA (Analysis of Variance) calculation demonstrated no significant difference among the τ values in 5 of the 7 tumors for each group ($P>0.5$). The fact that $\tau(SaO_2)$ is a little larger than $\tau_1(\Delta HbO_2)$ is possibly due to a narrower instrument bandwidth of the pulse oximeter than that of the NIRS system. Conversely, $\tau_2(\Delta HbO_2)$ has a relatively large value with a large deviation (~14±11 minutes). We may speculate that this slow, gradual elevation results from the venous or poorly perfused regions, where the vessels are much less sensitive to the intervention. The difference in response to carbogen (bi-phasic) and oxygen (mono-phasic) may arise from subtle effects of the vasoactive CO_2 components, causing delayed hemodynamic effects, and the effects showed considerable variability for individual tumors. The fact that $\tau(\Delta pO_2)$ is between $\tau_1(\Delta HbO_2)$ and $\tau_2(\Delta HbO_2)$ suggest that the dynamic changes in tumor pO_2 occur, while both well perfused and poorly perfused regions are undergoing oxygenation, overlapping the fast and slow perfusions.

Another observation is that the time delays of the three measured signals with respect to the initial time of the gas switch have the temporal order of $t_d(SaO_2) < t_d(\Delta[HbO_2]) < t_d(\Delta pO_2)$. Logically, switching to hyperoxic gas caused the systemic arterial SaO_2 to increase as a result of the immediate combination of deoxyhemoglobin with oxygen in high-pO_2 arterial blood. The highly oxygenated blood circulated in the systemic vasculature of the rats, including the capillary bed in the tumor tissue, resulting in a delayed increase in $[HbO_2]$ in the tumor vasculature and leading to an unloading of oxygen to the tumor tissue. The released oxygen diffused to the tumor tissue, yielding a more delayed elevation of tissue pO_2 in the tumor.

Inhalation of hyperoxic gases was considered to be one of the most effective methods to reduce tumor hypoxia, and thus, to enhance the efficiency of standard therapies in experimental malignancies as well as in human tumors. Carbogen has been favored over oxygen as an adjuvant intervention to enhance non-surgical therapy, and it has been suggested that oxygen breathing is less effective due to hypotension. Studies on experimental tumors in animals as well as on clinical trials in patients have shown non-uniform results, concerning the therapeutic benefit of the two kinds of respiratory hyperoxic gases[23,24,25,26], though all our results to date in various experimental rat prostate and breast tumors have suggested similar effects of oxygen or carbogen inhalation on pO_2[27]. The effects of carbogen and oxygen interventions on $\Delta[HbO_2]$ were compared using two groups of rat breast tumors in different inhalation sequences. The results have shown that both carbogen and oxygen can significantly improve the oxygen status of the tumors ($p<0.0001$) (Figs.6 and 9). Although the mean of the maximal $\Delta[HbO_2]$ readings with oxygen intervention (~0.8±0.1) appeared greater than that with carbogen intervention (~0.7±0.1), independent of inhalation sequence (Fig.8 and 10), there was no significant difference ($p>0.3$).

The results in this study are consistent with our pervious work[18,20], but now with a much larger group of breast tumors. The effects of carbogen and oxygen intervention on tumor oxygenation are in good agreement with those reported by Thews et al[28] although the prolonged effect of carbogen inhalation on tumor oxygenation after its cessation did not appear in our study.

The FOXY™ fiber optic, oxygen-sensing system offers a new alternative means for real-time monitoring of pO_2 in tumors. Compared with the pO_2 electrode used in our pervious work[20], the FOXY™ system confirms the heterogeneity of the tumors: now with several probes simultaneously in multiple regions in the tumors. Probes may be moved to search for representative high and low pO_2 baseline regions so as to sample diverse dynamic responses. In

essences, FOXY™ is a low cost version of OxyLite™, which we have used previously in prostate tumors[29]. We are confident in the measures of ΔpO_2, but unlike the Oxylite™, evaluation of absolute values of pO_2 awaits further validation. Ultimately, electrode or optical probe methods sample very limited regions compared with the ^{19}F MR technique. FREDOM can image a pO_2 map of 50–150 individual locations to display the heterogeneity of tumor oxygenation[15,29].

In this study, tumor volumes do not show any direct relationship with time constants or changes of amplitude in response to hyperoxic gas interventions. One possible reason is because time constant or order of magnitude analysis is relatively insensitive to the size and boundary conditions of the sample under study[21].

In conclusion, the ability of the NIRS to monitor therapeutic interventions for rat breast tumors *in-vivo* in real time has been demonstrated. We compared simultaneous measurements of SaO_2, $[HbO_2]$, and pO_2 of 14 rat breast tumors to evaluate their dynamic responses to carbogen and oxygen challenges. The response times were quantified by the time constants of the exponential fitting curves, showing the fastest response from the arterial SaO_2, followed by tumor vascular $[HbO_2]$, and further delayed responses for pO_2. The biphasic dynamic feature of $\Delta[HbO_2]$ suggests two different perfusion mechanisms in the tumor vasculature. The results in comparison for the effects of carbogen and oxygen intervention have demonstrated that both of the gases can significantly improve the tumor oxygen status without significant difference. However, the biphasic characteristic of $\Delta[HbO_2]$ with carbogen intervention disappeared in most of the cases in the "reverse" inhalation sequence. Heterogeneous responses to hyperoxic interventions in the tumor were displayed by the pO_2 signals measured in different regions of the

tumor. This study supports that the NIRS system can be a potentially useful monitoring means in cancer research and perhaps in clinical cancer applications.

ACKNOWLEDGEMENT

This work was supported in part by the Department of Defense Breast Cancer Research grants BC000833 (YG) and BC990287 (HL), and NIH RO1 CA79515 (RPM) and RO1 supplement CA79515(VB). We are grateful to Mengna Xia and Dr. Dawen Zhao for assistance with data processing. We gratefully acknowledge Dr. Weina Cui for helpful discussion.

Legend for the illustrations:

Figure 1. Schematic diagram of experimental setup for the NIR spectroscopy system, FOXY™ fiber optic, oxygen-sensing system and a pulse oximeter. In the NIR system, the 3 mm-diameter fiber bundles deliver and detect the laser light through the tumor in transmittance geometry. PMT represents a photomultiplier tube. I/Q is an in-phase and quadrature phase demodulator for retrieving amplitude and phase information. In the FOXY™ system, three fiber optic oxygen-sensing needles were inserted in different regions of the tumor. The probe of the pulse oximeter was placed on the hind foot of the rat.

Figure 2. The time profile of the three oxygen-sensitive parameters, i.e., normalized vascular oxy-hemoglobin concentration changes, $\Delta[HbO_2]$, mean tumor tissue partial pressure changes, ΔpO_2, and arterial oxygen saturation, SaO_2, with respect to carbogen intervention in a representative 13762NF rat breast tumor (No.1, 3.2 cm^3).

Figure 3. Responses of the three oxygen-sensitive parameters to carbogen intervention in the rising part. Single-exponential fittings yielded: $SaO_2 = 0.204\{1-\exp[-(t-20.02)/1.1]\}+0.85$ with $R=0.93$, $\Delta[HbO_2]= 0.655\{1-\exp[-(t-20.36)/2.59]\}+0.125$ with $R=0.89$, and $\Delta pO_2 =42.68\{1-\exp[-(t-21.01)/4.56]\}+16.66$ with $R=0.98$; Two-exponential fitting resulted in $\Delta[HbO_2]= 0.373(1-\exp(-(t-20.36)/0.61)+ 0.648(1-\exp(-(t-20.36)/21)$ with $R=0.97$.

Figure 4. Differences of time constants, τ, for SaO_2, ΔpO_2 with respect to $\Delta[HbO_2]$ in the five breast tumors. The circle symbols represent $\tau(SaO_2)$-$\tau(\Delta[HbO_2])$, and the triangle symbols indicate $\tau(\Delta pO_2)$-$\tau(\Delta[HbO_2])$.

Figure 5. Time delays of SaO_2, ΔpO_2 with respect to $\Delta[HbO_2]$ after the onset of gas intervention in the five breast tumors. The solid circles and triangles represent the response time delays of ΔpO_2 with respect to $\Delta[HbO_2]$ in the rising and falling part of the intervention, respectively. All the values are positive. The open circles and triangles indicate the response time delays of SaO_2 with respect to $\Delta[HbO_2]$ in the rising and falling part of the intervention, respectively. Almost all of the values are negative.

Figure 6. Time course of tumor vascular $\Delta[HbO_2]$ for a representative 13762NF breast tumor (No.2, 3.0cm^3) with the inhaled gas under the first sequence of air-carbogen-air-oxygen-air.

Figure 7. Comparison of the effects of carbogen and oxygen intervention on $\Delta[HbO_2]$ in a breast tumor (No.2, 3.0 cm^3). Single-exponential fitting yielded: $\Delta[HbO_2]=0.667\{1-\exp[-(t-20.01)/3.40]\}+0.167$ (R=0.91) for carbogen intervention; $\Delta[HbO_2]=0.57\{1-\exp[-(t-60.01)/0.51]\}+0.33$ (R=0.91) for oxygen intervention. Two-exponential fitting for carbogen inhalation yielded: $\Delta[HbO_2]=0.23\{1-\exp[-(t-20.01)/0.62]\}+0.486\{1-\exp[-(t-20.01)/11]\}+0.33$ (R=0.96).

Figure 8. Average maximal values of normalized $\Delta[HbO_2]$ for the seven breast tumors with gas inhalations for the sequence of air-carbogen-air-oxygen-air.

Figure 9. Time course of tumor vascular $\Delta[HbO_2]$ for a representative 13762NF breast tumor (No.9, 2.6 cm^3) under the second sequence of the "reversed" gas inhalation: air-oxygen-air-carbogen-air.

Figure 10. Average maximal values of normalized $\Delta[HbO_2]$ for the seven breast tumors with the gas inhalations under the sequence of air-oxygen-air-carbogen-air.

Figure 11. Time profiles of tumor oxygen tension changes, ΔpO_2, measured with the three channels of the FOXY™ fiber optic, oxygen-sensing system with respect to different gas inhalations on a breast tumor (No.3, 4.6 cm^3). The mean signal over the three channels was calculated as an arithmetical mean of the three curves and is plotted by the thicker trace.

Reference

[1] R.S. Bush, R.D.T. Jenkin, W.E.C Allt, F.A. Beale, A.J. Dembo, J.F. Pringle, "Definitive evidence for hypoxic cells influencing cure in cancer therapy". Br. J Cancer.**37(suppl 3)**,302-306 (1978).

[2] E.J. Hall, Radiobiology for the radiologist. 4th ed.(Lippincott, Philadelphia, PA.,1994).

[3] M .Nordsmark, J. Overgaard , "A confirmatory prognostic study on oxygenation status and loco-regional control in advanced head and neck squamous cell carcinoma treated by radiation therapy". Radiother Oncol.**57**,39-43 (2000).

[4] O. Thews, D.K. Kelleher, P. Vaupel, " Erythropoietin restores the anemia-induced reduction in cyclophosphamide cytotoxicity in rat tumors," Cancer Res,**61**,1358-1361 (2001).

[5] J. H.A..M. Kaanders, L.A.M. Pop, H.A.M. Marres, R.W.M.van der Maazen, A.J.van der Kogel and W.A.J.van Daal, "Radiotherapy with carbogen breathing and nicotinamide in head and neck cancer: feasibility and toxicity,".Radiother Oncol.**37**:190-198 (1995).

[6] M.I.Saunders, P.J.Hoskin, K.Pigott, "Accelerated radiotherapy, carbogen and nicotinamide (ARCON) in locally advanced head and neck cancer: a feasibility study," Radiother Oncol.**45**,159-166 (1997).

[7] J.A.Kruuv, W.R.Inch, J.A.McCredie, "Blood flow and oxygenation of tumors in mice. I. Effects of breathing gases containing carbon dioxide at atmospheric pressure," Cancer.**20**,51-59 (1967).

[8] H.B.Stone, J.M.Brown ,T.Phillips and R.M.Sutherland, "Oxygen in human tumors: correlations between methods of measurement and response to therapy", Radiat.Res., **136**,422-434 (1993).

[9] R.A.Gatenby, H.B.Kessler, J.S.Rosenblum, L.R.Coia, P.J.Moldofsky, W.H.Hartz, G.J.Border,"Oxygen distribution in squamous cell carcinoma metastases and its relationship to the outcome of radiation therapy," Int.J.Radiat. Oncol.Biol.Phys.**14**,831-838 (1988).

[10] W.M.Klieser,K.H.Schlenger,S.Walenta,M.Gross, U. Harbach, M. Hoekel, " Pathophysiological approaches to identifying tumor hypoxia in patients," Radiother. Oncol. **20**(suppl) 21-28 (1991).

[11] S.M.Evans,S.Hahn, D.R.Pook, W.T.Jenkins,A.A.Chalian, P.Zhang, C.Stevens, R.Weber,G.Weinstein and I.Benjamin, "Detection of hypoxia in human squamous cell carcinoma by EF5 binding", Cancer Res. **60**, 2018-2024 (2000).

[12] J.A.Raleigh, S.C.Chou, D.P.Calkins-Adams, C.A.Ballenger, D.B.Novotny and M.A.Varia, "A clinical study of hypoxia and metallothionein protein expression in squamous cell carcinomas". Clin.Cancer Res. **6**, 855-862 (2000).

[13] E.K.Rofstad, P.DeMuth, B.M.Fenton, R.M.Sutherland, "^{31}P NMR spectroscopy studies of tumor energy metabolism and its relationship to intracapillary oxyhemoglobin saturation status and tumor hypoxia," Cancer Res. **48**:5440-5446 (1988).

[14] R.P.Mason, P.P.Antich, E.E.Babcock, A.Constantinescu, P.Peschke, E.W.Hahn, "Noninvasive determination of tumor oxygen tension and local variation with growth," Int.J.Radiat. Oncol. Biol.Phys. **29**,95-103 (1994).

[15] D.Zhao, A.Constantinescu, L.Jiang, E.W.Hahn, R.P.Mason, "Prognostic radiology:quantitative assessment of tumor oxygen dynamics by MRI," Am. J. Clin Oncol. **24(5)**,462-466 (2001).

[16] E.L.Hull, D.L. Conover, and T.H. Foster, "Carbogen induced changes in rat mammary tumor oxygenation reported by near infrared spectroscopy," Br.J.Cancer. **79**,1709-1716 (1999).

[17] H.Liu, Y.Song, K. L.Worden, X.Jiang, A.Constantinescu, and R.P.Mason, " Noninvasive investigation of blood oxygenation dynamics of tumors by near-infrared spectroscopy," Appl. Opt. **39**,5231-5243 (2000).

[18] Y.Gu, Z.Qian, J.Chen, D.Blessington, N.Ramanujam ,and B.Chance, "High resolution three dimensional scanning optical image system for intrinsic and extrinsic contrast agents in tissue," Rev. Sci. Instrum.**73**, 172-178 (2002).

[19] J.G.Kim, Y.Song, D.Zhao, A.Constantinescu, R.P.Mason, and H.Liu, "Interplay of Tumor Vascular Oxygenation and pO_2 in Tumors Using NIRS, ^{19}F MR pO_2 Mapping, and pO_2 Needle Electrode," J. Biomed. Optics (accepted for publication) 2002.

[20] E.W.Hahn,P.Peschke,R.P.Mason, E.E.Babcock and P.P.Antich, "Isolated tumor growth in a surgically formed skin pedicle in the rat: A new tumor model for NMR studies", Magn.Reson. Imaging **11**, 1007-1017 (1993).

[21] E.N.Lightfoot, K.A.Duca, "The roles of mass transfer in tissue function " in *The Biomedical Engineering Handbook, second edition. Section XII ,Tissue Engineering* , J.Bronzino.(CRC Press LLC, Florida, 2000), P 115-6.

[22] H. Liu, A. H. Hielscher, F. K. Tittel, S. L. Jacques, and B. Chance, "Influence of Blood Vessels on the Measurement of Hemoglobin Oxygenation as Determined by Time-Resolved Reflectance Spectroscopy," Med. Phys. **22**, 1209-1217 (1995).

[23] S. Dische, "What we learnt from hyperbaric oxygen?" Radiother oncol.**20**(suppl),71-74(1991).

[24] S.Dische, M.I.Saunders, R.Sealy, "Carcinoma of the cervix and the use of hyperbaric oxygen with radiotherapy:a report of a randomized controlled trial," Radiother Oncol.**53**,93-98 (1999).

[25] V.M.Laurence, R.Ward, I.F.Dennis, N.M.Bleehen, "Carbogen breathing with nicotinamide improves the oxygen status of tumors in patients," Br. J Cancer,**72**,198-205 (1995).

[26] L.Martin, E.Lartigau, P.Weeger, "Changes in the oxygenation of head and neck tumors during carbogen breathing," Radiother Oncol,**27**,123-130 (1993).

[27] S., Hunjan, D.Zhao, A.Constantinescu, E.W.Hahn , P.P.Antich, R.P.Mason, "Tumor oximetry: demonstration of an enhanced dynamic mapping procedure using Fluorine-19 echo planar magnetic resonance imaging in the Dunning prostate R3327-AT1 rat tumor", Int. J. Radiation Oncology Biol. Phys., **49**, 1097-1108 (2001).

[28] O.Thews, D.K.Kelleher, P.Vaupel. "Dynamics of tumor oxygenation and red blood cell flux in response to inspiratory hyperoxia combined with different levels of inspiratory hypercapnia," Radiother. Oncol., **62**, 77-85 (2002).

[29] D.Zhao, A.Constantinescu, E.W.Hahn ,R.P.Mason, "Tumor oxygen dynamics with respect to growth and respiratory challenge: Investigation of the Dunning Prostate R3327-HI Tumor," Radiat. Res. **156**, 510-520 (2001).

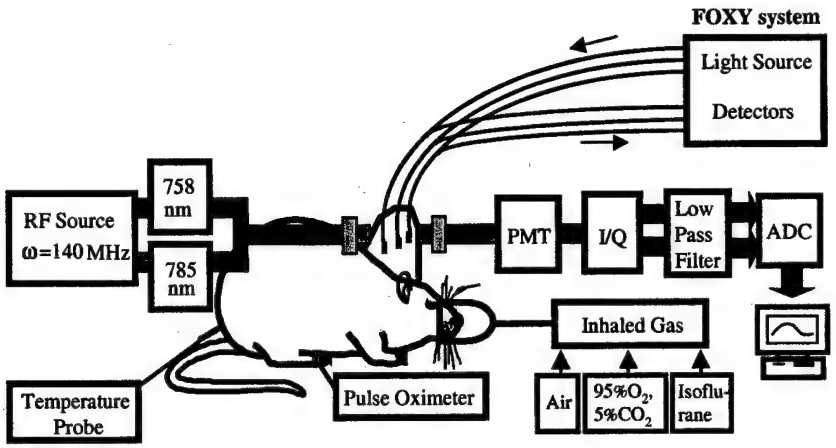

Figure 1. Schematic diagram of experimental setup for the NIR spectroscopy system, FOXY™ fiber optic, oxygen-sensing system and a pulse oximeter. In the NIR system, the 3 mm-diameter fiber bundles deliver and detect the laser light through the tumor in transmittance geometry. PMT represents a photomultiplier tube. I/Q is an in-phase and quadrature phase demodulator for retrieving amplitude and phase information. In the FOXY™ system, three fiber optic oxygen-sensing needles were inserted in different regions of the tumor. The probe of the pulse oximeter was placed on the hind foot of the rat.

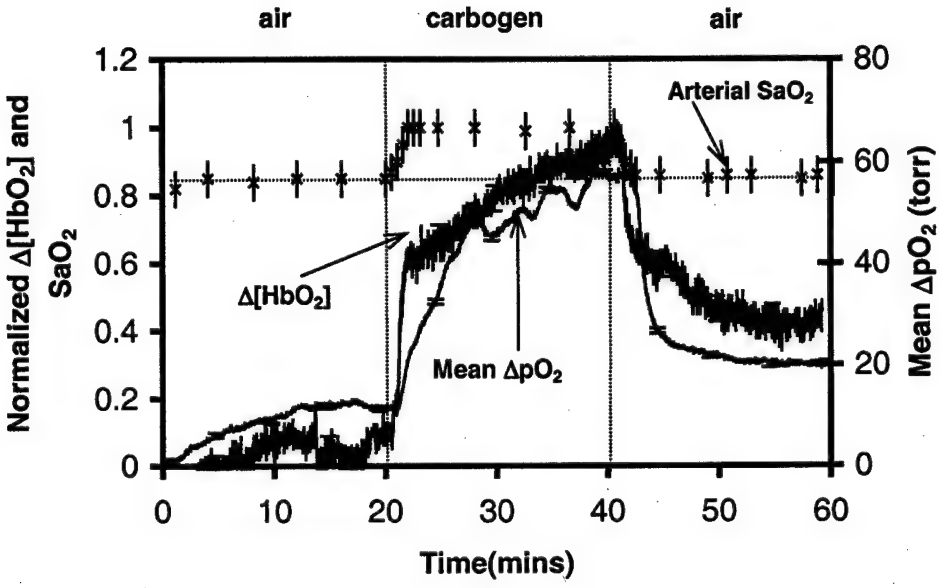

Figure 2. The time profile of the three oxygen-sensitive parameters, i.e., normalized vascular oxy-hemoglobin concentration changes, $\Delta[HbO_2]$, mean tumor tissue partial pressure changes, ΔpO_2, and arterial oxygen saturation, SaO_2, with respect to carbogen intervention in a representative 13762NF rat breast tumor (No.1, 3.2 cm^3).

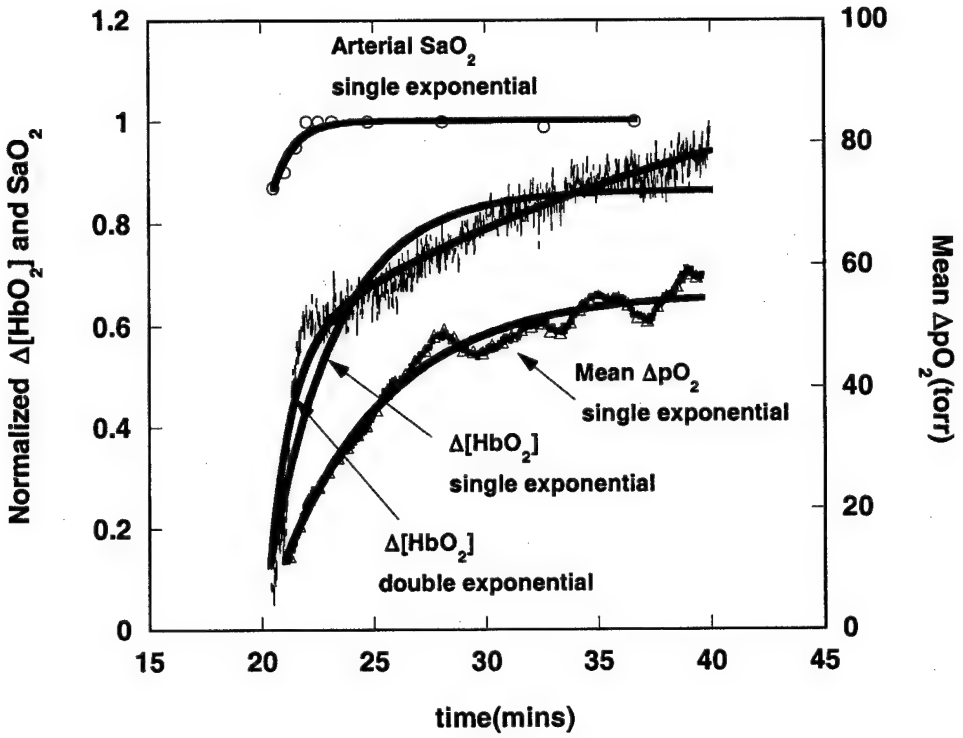

Figure 3. Responses of the three oxygen-sensitive parameters to carbogen intervention in the rising part. Single-exponential fittings yielded: SaO_2 = 0.204{1-exp[-(t-20.02)/1.1]}+0.85 with R=0.93, $\Delta[HbO_2]$= 0.655{1-exp[-(t-20.36)/2.59]}+0.125 with R=0.89, and ΔpO_2 =42.68{1-exp[-(t-21.01)/4.56]}+16.66 with R=0.98; Two-exponential fitting resulted in $\Delta[HbO_2]$= 0.373(1-exp(-(t-20.36)/0.61)+ 0.648(1-exp(-(t-20.36)/21) with R=0.97.

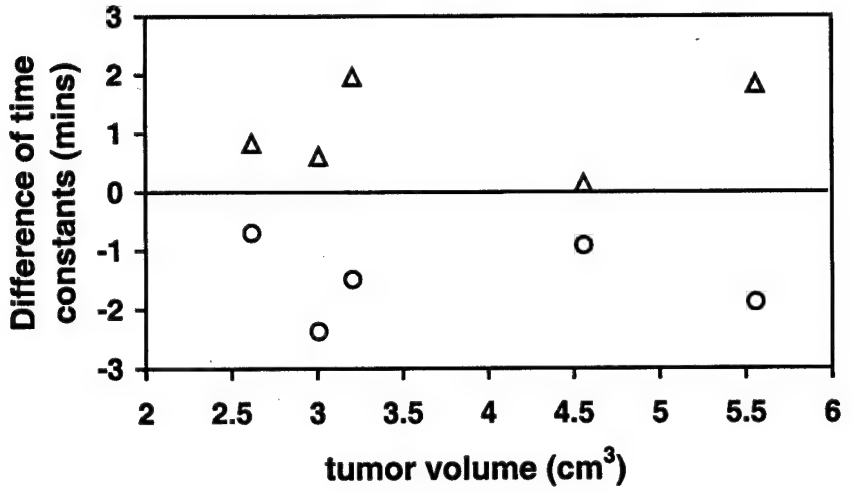

Figure 4. Differences of time constants,τ, for SaO_2, ΔpO_2 with respect to $\Delta[HbO_2]$ in the five breast tumors. The circle symbols represent $\tau(SaO_2)$-$\tau(\Delta[HbO_2])$, and the triangle symbols indicate $\tau(\Delta pO_2)$-$\tau(\Delta[HbO_2])$.

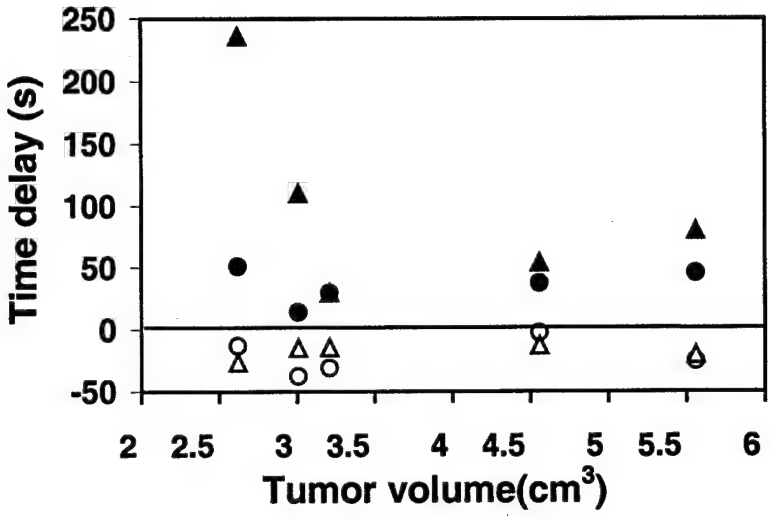

Figure 5. Time delays of SaO_2, ΔpO_2 with respect to $\Delta[HbO_2]$ after the onset of gas intervention in the five breast tumors. The solid circles and triangles represent the response time delay of ΔpO_2 with respect to $\Delta[HbO_2]$ in the rising part and falling part of the intervention, respectively. All the values are positive. The hollow circles and triangles indicate the response time delay of SaO_2 with respect to $\Delta[HbO_2]$ in the rising and falling part of the intervention, respectively. All the values are negative.

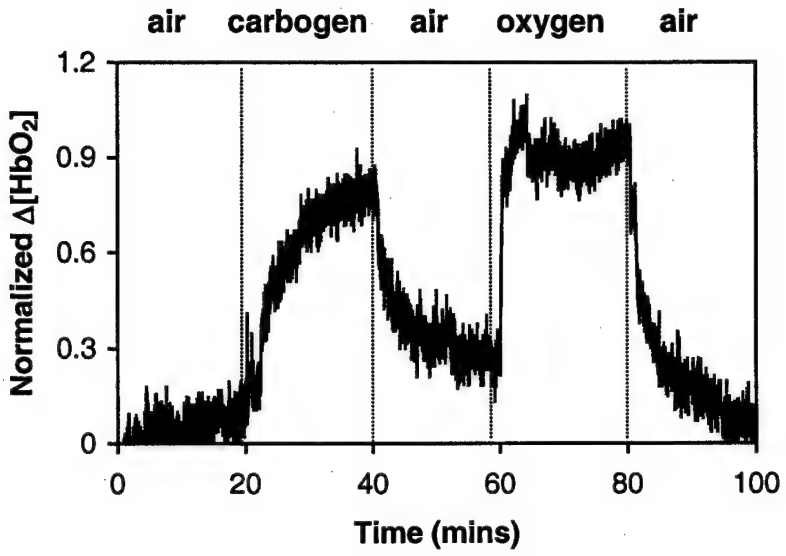

Figure 6. Time course of tumor vascular $\Delta[HbO_2]$ for a representative 13762NF breast tumor (No.2, 3.0cm^3) with the inhaled gas under the first sequence of air-carbogen-air-oxygen-air.

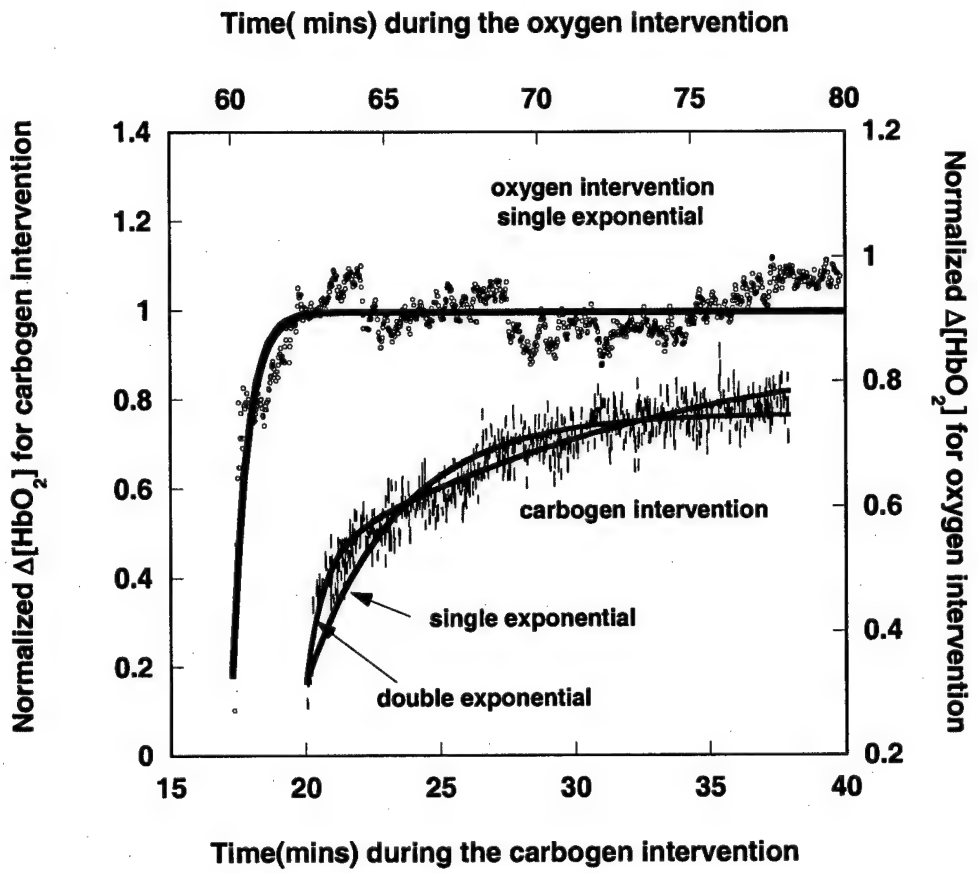

Figure 7. Comparison of the effects of carbogen and oxygen intervention on $\Delta[HbO_2]$ in a breast tumor (No.2, 3.0 cm^3). Single-exponential fitting yielded: $\Delta[HbO_2]=0.667\{1-\exp[-(t-20.01)/3.40]\}+0.167$ (R=0.91) for carbogen intervention; $\Delta[HbO_2]=0.57\{1-\exp[-(t-60.01)/0.51]\}+0.33$ (R=0.91) for oxygen intervention. Two-exponential fitting for carbogen inhalation yielded: $\Delta[HbO_2]=0.23\{1-\exp[-(t-20.01)/0.62]\}+0.486\{1-\exp[-(t-20.01)/11]\}+0.33$ (R=0.96).

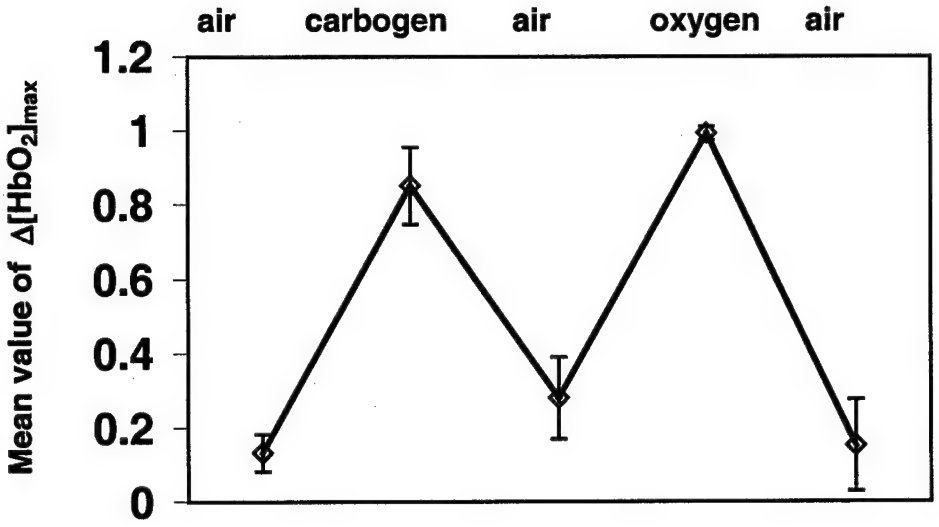

Figure 8. Average maximal values of normalized $\Delta[HbO_2]$ for the seven breast tumors with gas inhalations for the sequence of air-carbogen-air-oxygen-air.

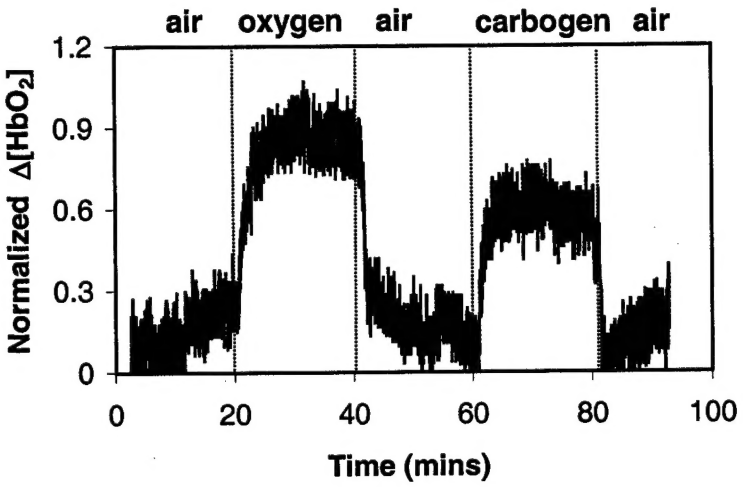

Figure 9. Time course of tumor vascular $\Delta[HbO_2]$ for a representative 13762NF breast tumor (No.9, 2.6 cm^3) under the second sequence of the "reversed" gas inhalation: air-oxygen-air-carbogen-air.

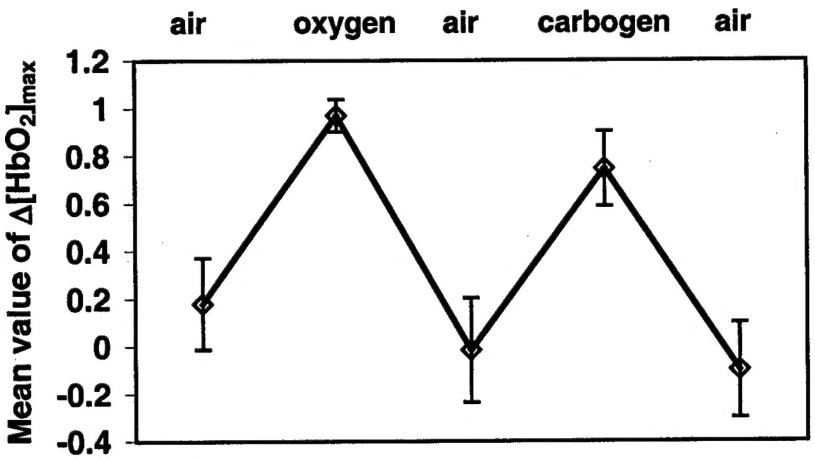

Figure 10. Average maximal values of normalized $\Delta[HbO_2]$ for the seven breast tumors with the gas inhalations under the sequence of air-oxygen-air-carbogen-air.

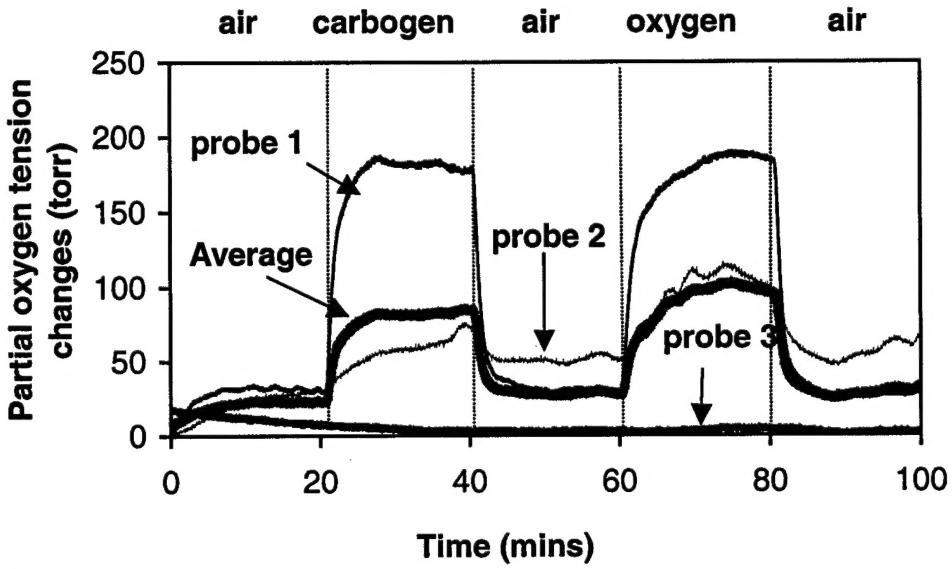

Figure 11. Time profiles of tumor oxygen tension changes, ΔpO_2, measured with the three channels of the FOXY™ fiber optic, oxygen-sensing system with respect to different gas inhalations on a breast tumor (No.3, 4.6 cm^3). The mean signal over the three channels was calculated as an arithmetical mean of the three curves and is plotted by the thicker trace.

Table I Time constants of SaO_2, $\Delta[HbO_2]$ and ΔpO_2 response to carbogen and oxygen intervention in the breast tumors; under the inhalation sequence of air-carbogen-air-oxygen-air.

Breast tumors volume (cm^3)	Single-exponential fitting of SaO_2, $\Delta[HbO_2]$ and ΔpO_2 (carbogen intervention)						Double-exponential fitting for $\Delta[HbO_2]$ (carbogen intervention)			Single-exponential fitting of $\Delta[HbO_2]$ (O_2 intervention)	
	SaO_2		$\Delta[HbO_2]$		ΔpO_2						
	τ (min)	R	τ (min)	R	τ (min)	R	τ1(min)	τ2(min)	R	τ(min)	R
No.1 (3.2)	1.1±0.2	0.93	2.59±0.06	0.89	4.56±0.04	0.98	0.61±0.03	21±3	0.97	0.35±0.01	0.92
No.2 (3.0)	1.6±0.2	0.98	3.40±0.07	0.91	4.6±0.1	0.82	0.62±0.06	11±1	0.96	0.51±0.01	0.91
No.3 (4.6)	1.2±0.2	0.97	2.12±0.06	0.76	2.26±0.02	0.98	0.6±0.1	37±3	0.96	1.52±0.02	0.89
No.4 (2.6)	1.9±0.3	0.98	2.68±0.05	0.93	3.5±0.1	0.86	0.12±0.02	5.2±0.1	0.98	1.71±0.03	0.94
No.5(5.6)	0.8±0.2	0.91	2.68±0.05	0.74	4.51±0.02	0.99	0.17±0.03	12.5±0.6	0.99	5.49±0.03	0.98
No.6 (1.9)	0.9±0.2	0.81	1.62±0.01	0.95	/	/	0.63±0.08	2.3±0.1	0.96	5.16±0.06	0.93
No.7(0.72)	1.0±0.5	0.95	3.60±0.03	0.93	/	/	0.61±0.02	10.5±0.3	0.98	3.54±0.03	0.95
Mean	1.2±0.4		2.7±0.6		4±1		0.5±0.2	14±11		2.5±2	